Dyes and Pigments 92 (2011) 633–641

Contents lists available at ScienceDirect

Dyes and Pigments

journal homepage: www.elsevier.com/locate/dyepig

Two-photon absorption dyes with thiophene as π electron bridge: Synthesis, photophysical properties and optical data storage

Hongping Zhou [a,*], Feixia Zhou [a], Shiya Tang [a], Peng Wu [a], Yixin Chen [a], Yulong Tu [a], Jieying Wu [a], Yupeng Tian [a,b,c]

[a] Department of Chemistry, Anhui University and Key Laboratory of Functional Inorganic Materials Chemistry of Anhui Province, 230039 Hefei, PR China
[b] State Key Laboratory of Crystal Materials, Shandong University, 250100 Jinan, PR China
[c] State Key Laboratory of Coordination Chemistry, Nanjing University, 210093 Nanjing, PR China

ARTICLE INFO

Article history:
Received 28 April 2011
Received in revised form
19 June 2011
Accepted 23 June 2011
Available online 6 July 2011

Keywords:
Thiophene
Linear absorption
Single-photon excited fluorescence
Two-photon excited fluorescence
Calculation
TPA data storage

ABSTRACT

Four novel dyes are prepared by thiophene as π bridge between carbazole central core and other terminal groups by Suzuki and Heck coupling reactions. These dyes are fully characterized by IR, ^{1}H NMR, ^{13}C NMR, MS and elemental analysis. Linear absorption, single- and two-photon excited fluorescence in various solvents are experimentally investigated. The calculated two-photon absorption cross sections of 9-Hexyl-3,6-di((5-phenyl)-2-thienyl)carbazole (**1**), 9-Hexyl-3,6-di((5-thienyl)-2-thienyl)carbazole (**2**), 9-Hexyl-3,6-di((5-p-vinylpyridyl)-2-thienyl)-carbazole (**3**) and 9-Hexyl-3,6-di-((5-o-vinylpyridyl)-2-thienyl) carbazole (**4**) for the lowest excited state are 537.84, 550.76, 1292.95 and 1340.40 × 10^{-50} cm^4 s $photon^{-1}$, respectively. Calculated and experimental data have shown that thiophene as π electron bridge improves the two-photon absorption cross sections greatly. Two-photon optical data recording experiments have been carried out at 820 nm laser radiation.

1. Introduction

Organic molecules that can simultaneously absorb two or more photons to be promoted to their excited states have recently been the subject of much research due to the growing interest in advanced photonic applications, such as optical limiting [1], three-dimensional optical storage [2], microfabrication [3], and up converted lasing [4]. To fully realize these applications, an intense worldwide effort has been focused on the design of organic materials with a large TPA cross section (δ) at desirable wavelengths. Up to now, several efficient design strategies have been put forward to enhancing δ_{TPA}, such as the π-conjugated was employed to connect donor (D) and acceptor (A) symmetrically or asymmetrically to form D–A–D, D–π–A, D–π–D, D–π–A and A–π–D–π–A structures, macrocycles, dendrimers, polymers and multibranched molecules. Furthermore, several other studies on structure–property relationship reveal that the δ_{TPA} increase with the D/A strength, chain length, and planarity of the π-center [5]. In recent years, some researchers get the information that the electron could interact through pseudo-conjugated system (σ system) between two π systems [6].

In order to obtain more information, we have designed a series of dyes with systematic molecular structure of types A–π–D–π–A and π–σ–π, where D is carbazole, A is pyridine, and π represents a π-conjugated vinyl or thiophene ring. The carbazolyl group is chosen due to its rigid plane, long conjugation length, good hole transporting properties and their charge transporting compounds creating free carriers in the visible region through the photo-carrier generation process, and thiophene-based π-conjugating spacers have been proved effective in photovoltaic cells because of their chemical and environmental stability as well as their electronic tunability [7].

In this paper, four novel dyes (**1**, **2**, **3** and **4**) were synthesized *via* Suzuki and Heck coupling reactions as illustrated in Scheme 1. Structural confirmation data for the four new dyes are presented. Linear absorption, steady-state fluorescence and two-photon absorption were measured. Our experimental and ability study results demonstrate that not only do the TPA cross sections of A–π–D–π–A (**3** and **4**) increase, but also those of π–σ–π type molecules (**1** and **2**) with introduction of thiophene ring increase.

Furthermore, we attempted to use the new dyes as optical data storage materials by the method of void creation in polymer

* Corresponding author. Tel.: +86 551 5108151; fax: +86 551 5107342.
E-mail addresses: zhpzhp@263.net, zhoufxfx@126.com (H. Zhou).

0143-7208/$ – see front matter © 2011 Elsevier Ltd. All rights reserved.
doi:10.1016/j.dyepig.2011.06.028

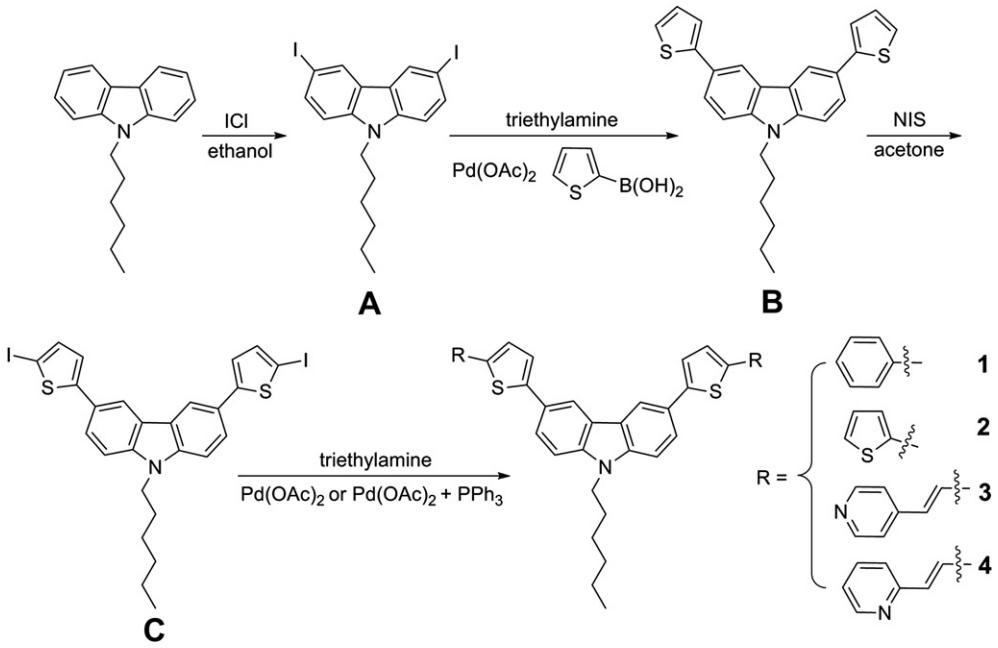

Scheme 1. Synthetic routes to four dyes **1**–**4**.

according to references [8]. The optical system that we used for data recording and reading with the new material was similar to the instrumental setup used in the polymerization [9]. Experimental results show the novel dyes exhibit good optical memory.

2. Experimental

2.1. Characterization

Elemental analyses were performed with a Perkins-Elmer 240 B instrument. IR spectra were recorded with a Nicolet FT-IR NEXUS 870 instrument (KBr discs) in the 4000–400 cm^{-1} region. ^1H NMR, ^{13}C NMR spectra were obtained on Bruker Avance 400 MHz spectrometer in $CDCl_3$ solution (with TMS as internal standard). Mass spectrum was determined with a Micro mass GTC-MS (EI source). The solvents were purified by conventional methods before use. The excitation source for the TPEF experiments was a mode-locked femtosecond Ti:Sapphire laser (Spectra-physics, 100 fs, 82 MHz) tuned to 720 nm. The maximum average laser power available for these experiments was about 100 mW. An optical streak camera was used as a recorder. All the samples are done by the concentration of 10^{-3} mol/L. The compounds and the methyl methacrylate resin were dissolved in CH_2Cl_2. Upon evaporation of the solvent at room temperature, the resin formed a film on a glass disk.

2.2. Synthesis

Considering thiophene is a better donor and can be readily functionalized in the 2- and/or 5-position, we prepared four new dyes by thiophene as π electron bridge between carbazole central core and other terminal groups by Suzuki and Heck coupling reaction. The synthetic route toward the four compounds is described in Scheme 1.

2.2.1. Intermediate *A*

Hexylcarbazole (2.51 g, 10 mmol) and ethanol (10 mL) were added to a three-necked flask equipped with a magnetic stirrer, a reflux condenser, an isobaric dropping funnel, ICl (5.00 g, 31 mmol)/ethanol (20 mL) was dropped to the mixture at 80 °C. The reaction mixture was refluxed for 2 h, cooled to room temperature and filtered. The product was crystallized with ethanol and produced pale blue crystals. Yield: 89.02%. IR (KBr, cm^{-1}) selected bands: 2947 (m), 2919 (s), 2848 (m), 1855 (w), 1718 (w), 1582 (w), 1467 (vs), 1424 (s), 1374 (m), 1342 (m), 1281 (s), 1227 (m), 1189 (w), 1145 (m), 1052 (w), 1003 (w), 856 (m), 795 (vs), 725 (m), 626 (m), 561 (m). ^1H NMR: ($CDCl_3$, 400 MHz), δ (ppm): 0.88 (s, 3H), 1.31 (s, 6H), 1.83 (t, J = 6.40 Hz, 2H), 4.23 (t, J = 7.20 Hz, 2H), 7.18 (d, J = 8.00 Hz, 2H), 7.73 (d, J = 8.40 Hz, 2H), 8.34 (s, 2H). ^{13}C NMR ($CDCl_3$, 100 MHz), δ (ppm): 13.985, 22.502, 26.876, 28.795, 31.500, 43.262, 81.637, 110.898, 123.984, 129.359, 134.498, 139.506. Anal. Calc. For $C_{18}H_{19}I_2N$: C, 42.97; H, 3.81; N, 2.78. Found: C, 42.58; H, 3.64; N, 2.36%. MS, m/z (%): 502.96 (M^+, 100), 431.87 ([M-n-C_5H_{11}]$^+$).

2.2.2. Intermediate *B*

A (3.00 g, 6 mmol) and DMF (10 mL) under nitrogen were added to a three-necked round-bottomed flask (80 mL) equipped with a magnetic stirrer, a reflux condenser and a nitrogen input tube. 10 mL of Et_3N was added until all of the precipitate dissolved at 70 °C. Thiophen-2-ylboronic acid (2.55 g, 20 mmol) and $Pd(OAc)_2$ were successively added, then the reaction mixture was refluxed in an oil bath at 130 °C under nitrogen. The reaction mixture was refluxed for 6 h and cooled to room temperature. The solution was dissolved in methylene chloride (200 mL), washed three times with distilled water, and dried with anhydrous magnesium sulfate. Then it was filtered and concentrated. The product was crystallized with ethyl acetate and gave dark yellow columnar crystals. Yield: 80.11%. IR (KBr, cm^{-1}) selected bands: 3417 (m), 3102 (m), 2963 (m), 2928 (m), 2849 (m), 1732 (s), 1684 (s), 1601 (s), 1484 (vs), 1424 (s), 1294 (s), 1234 (m), 1214 (m), 1160 (m), 1077 (w), 1047 (w), 865 (w), 826 (m), 800 (s), 694 (s). ^1H NMR: ($CDCl_3$, 400 MHz), δ (ppm): 0.92 (t, J = 7.20 Hz, 3H), 1.42–1.34 (m, 6H), 1.92–1.86 (m, 2H), 4.28 (t, J = 7.20 Hz, 2H), 7.17 (d, J = 4.00 Hz, 2H), 7.31 (d, J = 5.20 Hz, 2H), 7.39 (t, J = 4.40 Hz, 4H), 7.77 (d, J = 8.00 Hz, 2H), 8.38 (s, 2H). ^{13}C NMR ($CDCl_3$, 100 MHz), δ (ppm): 14.043, 22.563, 26.969, 29.013, 31.588, 43.330, 109.196,118.021, 122.138, 123.238, 123.727, 124.625, 125.939, 128.031, 140.449, 145.690. Calcd for $C_{26}H_{25}NS_2$: C, 75.14; H,

6.06; N, 3.37%. Found: C, 75.50; H, 6.39; N, 3.60%. MS, *m*/*z* (%): 415.14 (M^+, 100), 344.05 ([M-*n*-C_5H_{11}]$^+$), 262.07 ([M-*n*-C_5H_{11}–C_4H_3S]$^+$).

2.2.3. Intermediate ***C***

A round-bottomed flask (50 mL) equipped with a magnetic stirrer, was charged with B (0.13 g, 0.31 mmol) in acetone (9 mL). The reaction mixture was stirred at room temperature until all the precipitate was dissolved, and then NIS (0.42 g, 1.87 mmol) in acetone (4 mL) was added in portions. After 4 h of reflux, the reaction was checked by TLC (petroleum ether:ethyl acetate = 4:1) indicates that it was completed, and then dissolved in methylene chloride (200 mL), washed three times with distilled water and dried with anhydrous magnesium sulfate. Then it was filtered and concentrated. The solid was crystallized with ethanol and yellow acicular crystals were obtained. Yield: 54.21%. IR (KBr, cm^{-1}) selected bands: 3415 (s), 3234 (m), 2924 (w), 2849 (m), 1638 (s), 1616 (m), 1487 (w), 1384 (m), 802 (w), 623 (m). ^{1}H NMR: ($CDCl_3$, 400 MHz), δ (ppm): 0.90 (d, J = 7.20 Hz, 3H), 1.33 (t, J = 4.00 Hz, 6H), 1.87 (d, J = 7.20 Hz, 2H), 4.29 (t, J = 7.20 Hz, 2H), 7.04 (d, J = 4.00 Hz, 2H), 7.27 (d, J = 4.00 Hz, 2H), 7.39 (d, J = 8.40 Hz, 2H), 7.65 (q, J = 1.60 Hz, 2H), 8.23 (s, 2H). ^{13}C NMR ($CDCl_3$, 100 MHz), δ (ppm): 14.014, 22.534, 26.939, 28.984, 31.546, 43.377, 70.751, 109.351, 117.871, 123.133, 123.604, 124.452, 125.237, 137.911, 140.610, 151.608. Anal. Calc. For $C_{26}H_{23}I_2NS_2$: C, 46.79; H, 3.47; N, 2.10. Found: C, 46.43; H, 3.61; N, 2.32%. MS, *m*/*z* (%): 666.9 (M^+, 100), 595.85 ([M-*n*-C_5H_{11}]$^+$), 541.04 ([M − I]$^+$), 469.95 ([M − I-*n*-C_5H_{11}]$^+$).

2.2.4. 9-Hexyl-3, 6-di((5-phenyl)-2-thienyl)carbazole ***1***

Yellow powder was obtained by a similar method to B using C instead of A and benzene-2-ylboronic acid instead of thiophen-2-ylboronic acid. Compound **1** was purified by column chromatography on silica gel using petroleum ether as eluant. Yield: 53.23%. IR (KBr, cm^{-1}) selected bands: 3414 (m), 2957 (m), 2922 (m), 2850 (m), 1599 (s), 1482 (s), 1451 (s), 1385 (s), 1291 (m), 1240 (m), 1217 (w), 1156 (w), 799 (s), 748 (s), 687 (m). ^{1}H NMR: ($CDCl_3$, 400 MHz), δ (ppm): 0.91 (t, J = 6.00 Hz, 3H), 1.38 (m, 6H), 1.93 (t, J = 7.20 Hz, 2H), 4.34 (t, J = 7.20 Hz, 2H), 7.37–7.29 (m, 6H), 7.45–7.41 (m, 6H), 7.71 (q, J = 7.20 Hz, 4H), 7.80 (q, J = 1.60 Hz, 2H), 8.41 (s, 2H). ^{13}C NMR ($CDCl_3$, 100 MHz), δ (ppm): 14.009, 22.541, 26.965, 29.020, 31.571, 43.396, 109.272, 117.729, 122.976, 123.276, 124.046, 124.316, 125.522, 125.901, 127.242, 128.906, 134.593, 140.512, 142.433, 144.982. Calcd for $C_{38}H_{33}NS_2$: C, 80.38; H, 5.86; N, 2.47%. Found: C, 80.72; H, 6.24; N, 2.81%. MS, *m*/*z* (%): 567.2 (M^+, 100), 496.1 ([M-*n*-C_5H_{11}]$^+$).

2.2.5. 9-Hexyl-3, 6-di((5-thienyl)-2-thienyl)carbazole ***2***

Yellow powder was obtained by a similar method to B using C instead of A. Compound **2** was purified by column chromatography on silica gel using petroleum ether:ethyl acetate = 20:1 as eluant. Yield: 45.12%. IR (KBr, cm^{-1}) selected bands: 3422 (m), 2955 (m), 2922 (m), 2854 (w), 1602 (w), 1480 (w), 1454 (w), 1385 (s), 1237 (w), 794 (m), 761 (w), 692 (w). ^{1}H NMR: ($CDCl_3$, 400 MHz), δ (ppm): 0.90 (t, J = 6.80 Hz, 3H), 1.36 (m, 6H), 1.91 (t, J = 6.80 Hz, 2H), 4.31 (t, J = 6.80 Hz, 2H), 7.08 (d, J = 4.00 Hz, 2H), 7.25–7.21 (m, 6H), 7.30 (d, J = 4.00 Hz, 2H), 7.41 (d, J = 8.80 Hz, 2H), 7.75 (d, J = 8.80 Hz, 2H), 8.36 (s, 2H). ^{13}C NMR ($CDCl_3$, 100 MHz), δ (ppm): 14.024, 22.549, 26.960, 29.015, 31.569, 43.387, 109.308, 117.706, 122.663, 123.239, 123.282, 124.026, 124.285, 124.695, 125.631, 127.853, 135.554, 137.800, 140.509, 144.486. Calcd for $C_{34}H_{29}NS_4$: C, 70.42; H, 5.04; N, 2.42%. Found: C, 70.71; H, 5.34; N, 2.77%. MS, *m*/*z* (%): 579.1 (M^+, 100), 508.05 ([M-*n*-C_5H_{11}]$^+$).

2.2.6. 9-Hexyl-3, 6-di((5-p-vinylpyridyl)-2-thienyl)carbazole ***3***

A three-necked round-bottomed flask (80 mL) equipped with a magnetic stirrer, a reflux condenser and a nitrogen input tube, was charged with C (1.32 g, 2.00 mmol), DMF (30 mL) and water (10 mL) under a nitrogen atmosphere. Et_3N (10 mL) was added until all of the precipitate dissolved at 70 °C. 4-vinylpyridine (5 mL) was added and refluxed for 2 h, then PPh_3 (0.10 g, 0.38 mmol) and $Pd(OAc)_2$ (0.033 g, 0.15 mmol) were successively added. The mixture was allowed to warm to 90 °C. The mixture was refluxed for 6 h and cooled to room temperature. The solution is dissolved in methylene chloride (200 mL), washed three times with distilled water, and dried with anhydrous magnesium sulfate. Then it was filtered and concentrated. After removal the solvent, the residue was purified by column chromatography on a silica gel with petroleum ether/ethyl acetate (1:1) as eluant to yield pure red powder. Yield: 40.23%. IR (KBr, cm^{-1}) selected bands: 3551 (w), 3471 (m), 3412 (m), 2950 (m), 2925 (m), 2947 (m), 1017 (s), 1619 (m), 1593 (s), 1549 (w), 1439 (s), 1237 (w), 1206 (w), 1158 (w), 1136 (w), 1051 (w), 985 (w), 875 (w), 853 (w), 802 (s), 541 (m). ^{1}H NMR: (DMSO-d_6, 400 MHz), δ (ppm): 0.79 (t, J = 6.80 Hz, 3H), 1.25–1.15 (m, 6H), 1.78 (d, J = 6.00 Hz, 2H), 4.42 (t, J = 5.60 Hz, 2H), 6.92 (d, J = 16.00 Hz, 2H), 7.37 (d, J = 3.20 Hz, 2H), 7.55 (d, J = 5.20 Hz, 6H), 7.67 (d, J = 8.80 Hz, 2H), 7.83–7.74 (m, 4H), 8.53 (d, J = 4.80 Hz, 4H), 8.64 (s, 2H). ^{13}C NMR (DMSO-d_6, 100 MHz), δ (ppm): 14.278, 22.438, 26.514, 28.983, 31.391, 43.027, 110.794, 118.245, 119.950, 121.037, 121.229, 123.064, 123.754, 124.566, 124.653, 125.333, 127.134, 130.948, 139.889, 140.830, 144.562, 145.888, 150.411. Calcd for $C_{40}H_{35}N_3S_2$: C, 77.26; H, 5.67; N, 6.76%. Found: C, 77.62; H, 5.29; N, 6.45%. MS, *m*/*z* (%): 621.23 (M^+, 100), 550.10 ([M-*n*-C_5H_{11}]$^+$).

2.2.7. 9-Hexyl-3, 6-di((5-o-vinylpyridyl)-2-thienyl)carbazole ***4***

Yellow powder was obtained by a similar method to **3** using 2-vinylpyridine instead of 4-vinylpyridine. Compound **4** was purified by column chromatography on silica gel using petroleum ether:-ethyl acetate = 5:1 as eluant. Yield: 56.45%. IR (KBr, cm^{-1}) selected bands: 3466 (m), 3414 (m), 3061 (w), 2958 (m), 2925 (m), 2850 (m), 1622 (s), 1581 (s), 1559 (m), 1445 (m), 1423 (s), 1256 (s), 1199 (m), 1092 (s), 869 (m), 793 (m), 758 (w), 736 (m), 575 (w), 534 (m). ^{1}H NMR: ($CDCl_3$, 400 MHz), δ (ppm): 0.81 (t, J = 6.20 Hz, 3H), 1.40–1.20 (m, 6H), 1.84 (t, J = 6.80 Hz, 2H), 4.25 (t, J = 7.00 Hz, 2H), 7.14–6.92 (m, 6H), 7.25 (d, J = 3.60 Hz, 2H), 7.29 (d, J = 7.60 Hz, 2H), 7.35 (d, J = 8.40 Hz, 2H), 7.70 (d, J = 6.00 Hz, 2H), 7.71 (m, 4H), 8.31 (s, 2H), 8.54 (d, J = 4.80 Hz, 2H). ^{13}C NMR ($CDCl_3$, 100 MHz), δ (ppm): 14.012, 22.540, 26.951, 29.007, 31.558, 43.404, 109.355, 117.896, 121.789, 122.271, 122.753, 123.260, 124.436, 125.712, 126.739, 129.782, 136.347, 137.042, 140.303, 140.678, 146.052, 149.103, 155.143. Calcd for $C_{40}H_{35}N_3S_2$: C, 77.26; H, 5.67; N, 6.76%. Found: C, 77.64; H, 5.95; N, 6.37%. MS, *m*/*z* (%): 621.20 (M^+, 100), 550.20 ([M-*n*-C_5H_{11}]$^+$).

3. Results and discussion

3.1. Theoretical calculation

The electronic properties of dyes **1**–**4** have been investigated by means of theoretical calculations. The transition probability of OPA is given by oscillator strength

$$\delta_{op} = \frac{2\omega_f}{3}\sum_{\alpha}|\langle 0|\mu_\alpha|f\rangle|^2 \quad (1)$$

where $|0\rangle$ denotes the ground state, $|f\rangle$ the final state, ω_f the corresponding excitation frequency, and μ_α is the Cartesian component of the electronic dipole moment operator. The summation is performed over the molecular *x*, *y* and *z* axes.

The TPA cross section which can be directly comparable with experimental measurement is defined as

$$\sigma_{tp} = \frac{4\pi^2 a_0^5 \alpha}{15 c_0} \frac{\omega^2 g(\omega)}{\Gamma_f} \delta_{tp} \quad (2)$$

Here a_0 is the Bohr radius, c_0 is the speed of light, α is the fine structure constant, ω is the photon energy of the incident light, $g(\omega)$ denotes the spectral line profile, and Γ_f is the lifetime broadening of the final state, which is assumed to be 0.1 eV here [10]. δ_{tp} is written as follows [11]

$$\delta_{tp} = \sum_{\alpha\beta} \left[F \times S_{\alpha\alpha} S^*_{\beta\beta} + G \times S_{\alpha\beta} S^*_{\alpha\beta} + H \times S_{\alpha\beta} S^*_{\beta\alpha} \right] \quad (3)$$

where F, G and H are coefficients dependent on polarization of the light. $S_{\alpha\beta}$ is the TPA transition matrix element for the two-photon resonant absorption of identical energy, and can be written as [12]

$$S_{\alpha\beta} = \sum_j \left[\frac{\langle 0|\mu_\alpha|j\rangle\langle j|\mu_\beta|f\rangle}{\omega_j - \omega_f/2} + \frac{\langle 0|\mu_\beta|j\rangle\langle j|\mu_\alpha|f\rangle}{\omega_j - \omega_f/2} \right] \quad (4)$$

where α, $\beta \in (x, y, z)$, ω_j and ω_f are the excitation frequency for the intermediate state $|j>$ and the final state $|f>$, respectively.

The most straightforward approach to analyze optical properties of molecules is the response theory [13], which provides an analytical solution for the TPA cross section. The equilibrium geometries of molecules in gas phase are optimized by Gaussian package [14] at the hybrid density functional theory (DFT/B3LYP) level with 6-31G* basis set. The OPA and TPA properties are calculated by use of the response theory at DFT level implemented in DALTON [15].

In order to further investigate the electronic properties of **1**–**4** by means of theoretical calculations, we have plotted the HOMO and LUMO for dyes **1**–**4** in the gas phase, which is visualized by use of MOLEKEL program (pictures of HOMO–LUMO are available in Fig. 1). The HOMO is mainly located on the central carbazole ring in **1**–**4**, while the LUMO is localized on the central nodes and the linkages between those heterocycle and the carbazole ring for all dyes. Distributions of HOMO and LUMO levels are separated in all dyes indicating that the HOMO–LUMO transition can lead to charge-transfer.

The linear and nonlinear calculated optical properties for **1**–**4** in gas phase are listed in Table 1. The absorption maxima of the four dyes located from 343.25 to 401.08 nm, which correspond to $\pi-\pi^*$ transition for **1**–**2** but main CT transition for **3**–**4.** The energy gaps of the two-photon absorption band are almost equate to the energy gaps of the single-photon absorption band, which is tally with the theories of the nonlinear optics. From Table 1, one can observe that the calculated optical properties depend on the nature of the peripheral substituting groups due to their same principal framework part (9-hexyl-3, 6-bis(2-thienyl) carbazole). The responding field model is used to study the two-photon absorption cross section of the molecules. The largest two-photon absorption cross sections of molecules are 537.84 for **1**, 550.76 for **2**, 1292.95 for **3**, 1340.40 GM (1 GM = 10^{-50} cm^4 s photon^{-1}) for **4**, respectively, which is obviously increased in comparison with that of the intermediate **B** and the reported 3, 6-bis[2-(4-pyridyl)ethenyl]-9-ethylcarbazole (**L1**), 3, 6-bis[2-(2-pyridyl)ethenyl]-9-ethylcarbazole (**L2**) (Fig. 2) by our team performed based on the same TPA calculation [16]. Compounds **2**, **3** and **4** are different from **B**, **L1** and **L2** by one thiophene, and the TPA cross sections are increased equally by about 400 GM [16]. The results revealed that the thiophene as π electron bridge could increase δ_{TPA}, for both the $\pi-\sigma-\pi$, and A–π–D–π–A type molecules.

For the better understanding of the two-photon progress, we have plotted the charge density difference between the ground state and the first excited state (CT state) for **1**–**4** in the gas phase

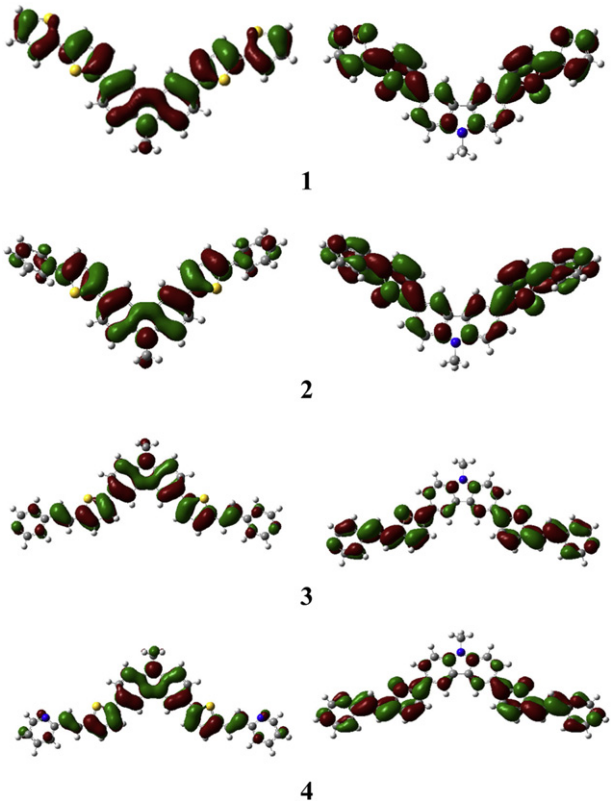

Fig. 1. HOMO and LUMO of **1**–**4** in the ground state (gas phase).

(see Fig. 3), which is visualized by the use of MOLEKEL program [17]. The blue pare represents where the electrons go and the gray pare represents where the electrons come from. For **1**–**4**, the CT plots are very similar. It can be seen that upon excitation, charges are mainly transferred from the two branches to the π-center. In the CT state, there is more electron density at the π-center on average, indicating that the molecule could be ready to give away its electron to its surrounding.

3.2. Linear absorption and single-photon excited fluorescence (SPEF)

The photophysical properties (absorption and fluorescence) of the new series of dyes in five different solvents (1.0×10^{-5} mol/L) are collected in Table 2 (including fluorescence quantum yields and lifetimes). Linear absorption spectra of **3** in toluene, THF, acetone, DMF and benzyl alcohol with a solution concentration of $c = 1.0 \times 10^{-5}$ mol/L are shown in Fig. 4. The linear absorption

Table 1
Calculated single- and two-photon-related photophysical properties of dyes **1**–**4** and intermediate **B** in gas phase.

Compd	ΔE_1[a]	$\lambda_{max}^{(1a)}$/nm[b]	ΔE_2[c]	$\lambda_{max}^{(2f)}$/nm[d]	δ[e]
B	4.41	280.81	4.35	568.53	177.51
1	3.61	343.25	3.87	639.05	537.84
2	3.40	364.35	3.66	675.72	550.76
3	3.09	401.08	3.26	785.63	1292.95
4	3.10	399.64	3.28	754.00	1340.40

[a] The energy gap of the single-photon absorption band.
[b] Peak position of the longest absorption band.
[c] The energy gap of the two-photon absorption band.
[d] Peak position of the two-photon absorption band.
[e] Two-photon absorption cross section in GM (1 GM = 10^{-50} cm^4 s photon^{-1}).

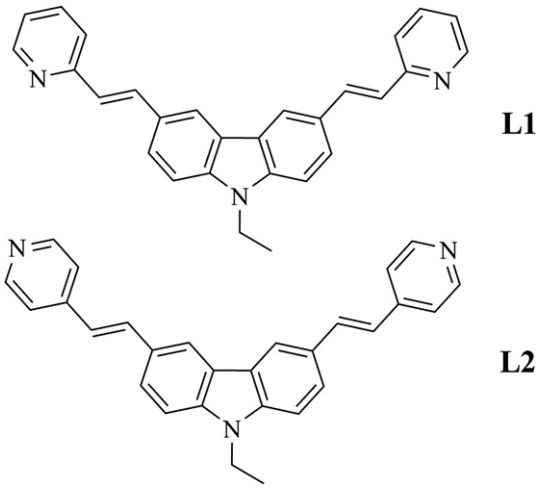

Fig. 2. Schematic drawing of **L1** and **L2**.

spectra of **3** are slightly red-shifted with the increasing solvent polarity and show little solvatochromic behavior. Table 2 shows the order of absorption maxima is **3** ≥ **4** > **2** > **1** in the same solvent. This confirms the fact that it flows of electrons through the thiophene ring than through a benzene ring [7,18,19]. The greater extent of π-electron delocalization makes an extraordinary bathochromic shift of the absorption band. Here, protonation of the pyridine group in **3** and **4** results in a much stronger electron-accepting group, thereby enhancing charge separation of π-electrons in the conjugated donor–acceptor structure [20]. The net effect of the protonation enhances ICT in benzyl alcohol comparing to the aprotic organic solvents such as acetone, THF and toluene,

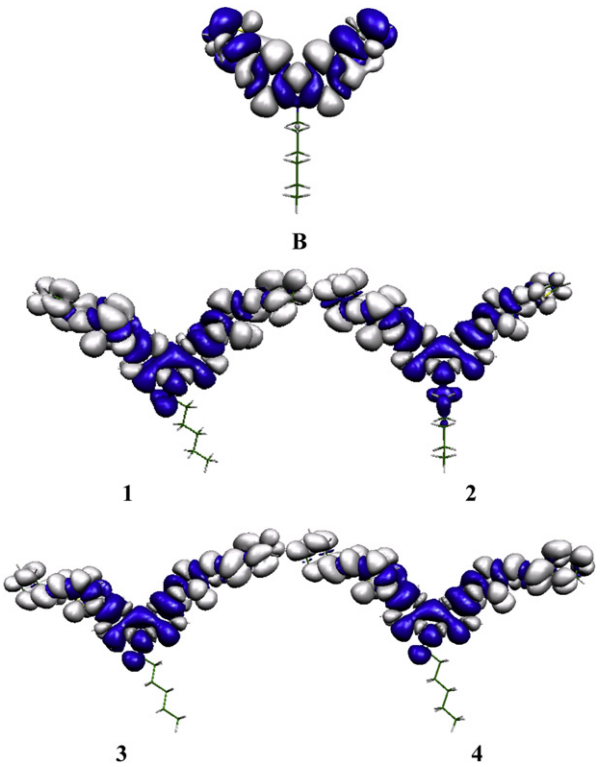

Fig. 3. Density difference between the charge-transfer and ground states of **1**–**4** in the gas phase.

Table 2
Photophysical properties of dyes **1**–**4** in several of different polar solvents.

Compd	Solvents	$\lambda_{max}^{(1a)}$/nm[a]	$\lambda_{max}^{(1f)}$/nm[b]	Φ[c]	$\Delta\nu$/cm^{-1}[d]
1	Toluene	344, 364	420, 435	0.068	3663
	THF	344, 364	425, 440	1.000	3831
	Acetone	344, 364	434	0.20	4431
	DMF	344, 369	442	0.15	4475
	Benzyl alcohol	344, 364	436	0.054	4536
2	Toluene	356, 379	426, 450	0.069	4163
	THF	359, 376	431, 449	0.778	4274
	Acetone	357, 374	446	0.069	4416
	DMF	358, 379	450	0.931	4163
	Benzyl alcohol	361, 376	438, 453	0.839	4520
3	Toluene	401	467	0.152	3524
	THF	401	500	0.044	4937
	Acetone	401	507	0.045	5213
	DMF	405	517	0.038	5348
	Benzyl alcohol	411	523	0.024	5210
4	Toluene	401	460	0.094	3198
	THF	401	482	0.090	4190
	Acetone	401	493	0.083	4653
	DMF	403	501	0.080	4853
	Benzyl alcohol	408	506	0.045	4746

[a] Peak position of the longest absorption band.
[b] Peak position of SPEF, exited at the absorption maximum.
[c] Quantum yields determined by using RhB and coumarin as standard.
[d] Stokes' shift in cm^{-1}.

which exhibits red shift to longer wavelength [21]. Protons from benzyl alcohol molecules can form hydrogen bond with the nitrogen heteroatom of pyridine rings and such hydrogen bond usually enhances charge separation.

However, with increasing polarity of the solvent, single-photon excited fluorescence (SPEF) spectra of all the dyes show remarkable bathochromic shifts. As shown in Fig. 5 and Table 2, for example, λ_{max} (SPEF) of **3** is located at 467 nm in toluene and red-shifted to 517 and 523 nm in DMF and benzyl alcohol, respectively. These results suggest that the molecule of the fluorescent exited state "assumed to be the first exited stated" S_1 must be larger than that of the ground state, as the enhanced dipole–dipolar interactions caused by the increasing polarity of solute and/or solvent will lead to a more significant energy level decrease for the exited state. In benzyl alcohol solution, it is the hydrogen bonds that stabilize the separated charge states.

The SPEF spectra of the dyes (**1**–**4**) at equimolar concentration were recorded in DMF solution (Fig. 6). Similar to absorption maxima, it can be seen that excited maxima is **3** ≥ **4** > **2** > **1** in DMF.

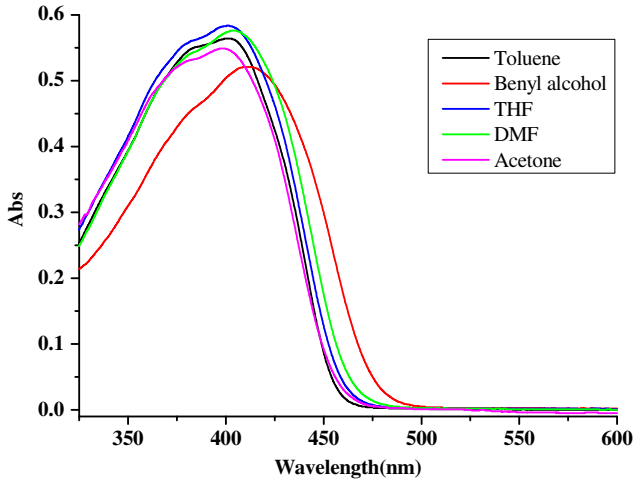

Fig. 4. Linear absorption spectra of **3** in five solvents.

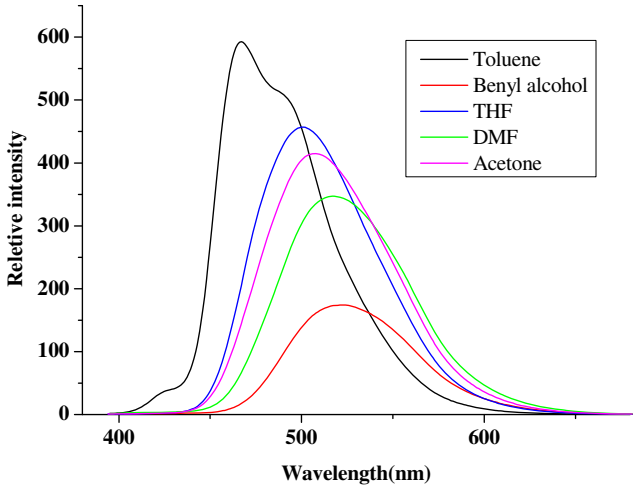

Fig. 5. Single-photon fluorescence spectra of **3** in five solvents with differing polarity.

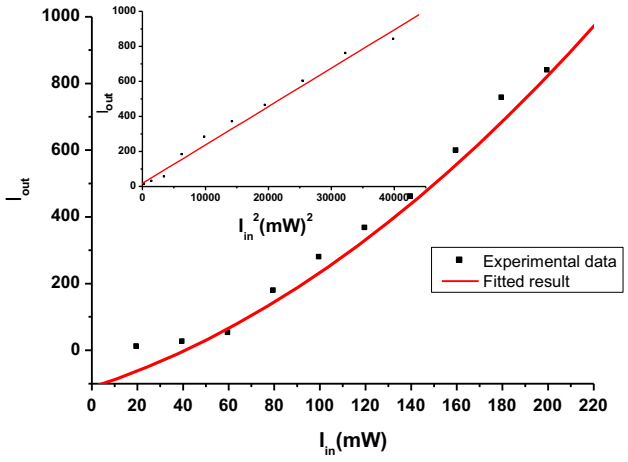

Fig. 7. Dependence of the output intensity (I_{out}) of compound **3** in DMF on the input laser power (I_{in}). The inset shows the linear dependence of I_{out} on I_{in}^2.

The quantum yields (Φ) of four compounds in different solvents were determined by using RhB for **1** and **2**, Coumarin for **3** and **4** as standard (Table 2). In order to further demonstrate the influence of solvent on fluorescence. Table 2 lists the Stokes' shift of the four dyes in solvents with different polarities. The Stokes' shift is defined as the loss of energy between absorption and reemission of light, which is a result of several dynamic processes. These processes include losses due to dissipation of vibrational energy, redistribution of electrons in the surrounding solvent molecules induced by the altered dipole moment of the excited dye, reorientation of the solvent molecules around the excited state dipole, and specific interactions between the fluorophore and the solvent or solutes. The Lippert equation is widely used to describe the effects of the physical properties of the solvent on the emission spectra of fluorophore [22].

$$\Delta\nu = \nu_{abs} - \nu_{em} = \left(2/cha^3\right)\Delta f\left(\mu_e - \mu_g\right)^2 + \text{const}$$

In this equation, h is Planck's constant, c is the speed of light, and a is the radius of the cavity in which the fluorophore resides. The wavenumbers of the absorption and emission are ν_a and ν_f (in cm^{-1}), respectively. In aprotic solvents, from Table 2, the Stokes' shifts are roughly approximately proportional to the orientation polarizability for all the four compounds, especially the Stokes' shifts of **3** and **4** are increased very rapidly with the increasing polarity. This is the typical characterization of CT correlating with abilities study [23].

3.3. TPA properties

As shown in Fig. 4, there is no linear absorption in the wavelength range 475–900 nm for **3**, which indicates that there are no energy levels corresponding to an electron transition in this spectral range. The linear dependence on the square of input laser power suggests a two-photon excitation mechanism at 750 nm for all the four molecules (Fig. 7). Fig. 8 shows TPEF of **1**–**4** in DMF at 750 nm excited wavelength. The peak wavelength of the TPEF is red-shifted relative to the SPEF for all the compounds, which is due to reabsorption in the high-concentrated solution. Fig. 9 shows that the TPEF of **3** in different solvents. It shows positive solvatochromism effect, the same trend as the one photon fluorescence. By tuning the pump wavelengths increment at 10 nm from 720 to 900 nm while keeping the input power fixed and then recording TPEF intensity, TPEF spectra are obtained.

TPA cross sections have been measured using fs TPEF in DMF. The obtained δ_{TPA} for **1** and **2** at 770 nm are 150 GM and 100 GM, the largest δ_{TPA} for **3** and **4** at 770 nm are 703 GM and 565 GM,

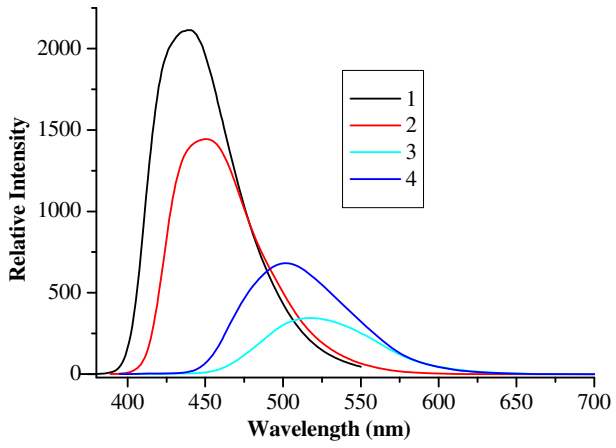

Fig. 6. Single-photon fluorescence spectra of **1**–**4** in DMF ($c = 1.0 \times 10^{-5}$ mol/L).

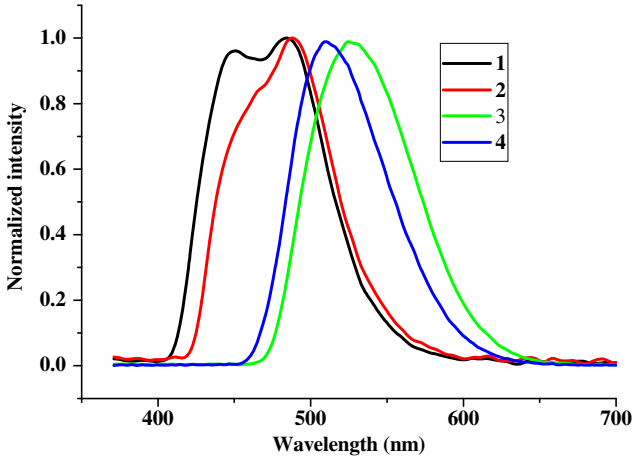

Fig. 8. Two-photon fluorescence spectra of **1**–**4** in DMF ($c = 1.0 \times 10^{-3}$ mol/L) at 750 nm excited wavelength.

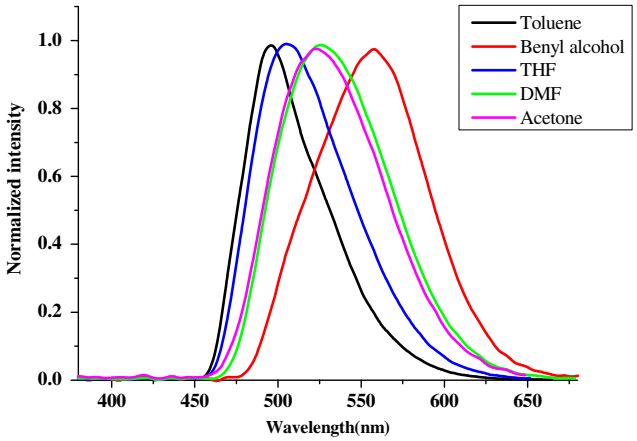

Fig. 9. The two-photon fluorescence spectra of **3** in five solvents with differing polarity ($c = 1.0 \times 10^{-3}$ mol/L).

respectively (Fig. 10). Considering the ideal molecules used in the calculation, it is easily to understand that the experimental values are smaller than the calculation results. Compared with the molecule we prepared before (**L1**), the calculation outcomes are acceptable. The experimental δ_{TPA} for **3** is larger than the one for the reported **L1**, by about 500 GM in experiment (703 GM for **3** *vs* 123 GM for **L1**) [16]. **L1** is different from **3** by one thiophene, the calculated value of **3** is also larger than that of **L1** (1292.95 GM for **3** *vs* 947 GM for **L1**). In conclusion, system with thiophene ring can greatly enhance the TPA cross sections. Previous reports show the contribution to TPA cross sections per double bonds is 155 GM at most. Here, we get the information that donor group thiophene is an effective 'electron bridge' that increases TPA cross sections [24].

3.4. TPA data storage

For the sake of long time storage, the materials must be doped into polymer. A polymer material has a low threshold of optical damage and provides the possibility of doping with absorbing dyes, which would allow the use of a long excitation wavelength to reduce the scattering effect and the manipulation of the refractive index. Poly(methyl methacrylate) (PMMA) is an interesting material because of its high chemical resistance, advantageous optical properties, and low cost. Recently, PMMA and dye-doped PMMA are extensively studied with respect to fs laser machining [8]. A recent publication by Yamasaki et al. [8] demonstrates the formation of voids in an undoped PMMA film by the use of single-shot ultrashort pulses with a wavelength of 400 nm. It has been shown that the voids in the PMMA can be read out under two-photon excitation. Moreover, Day and Gu [8] reported on the formation of submicrometer voids within dye-doped PMMA under multiphoton absorption (MPA) excited by an infrared laser beam.

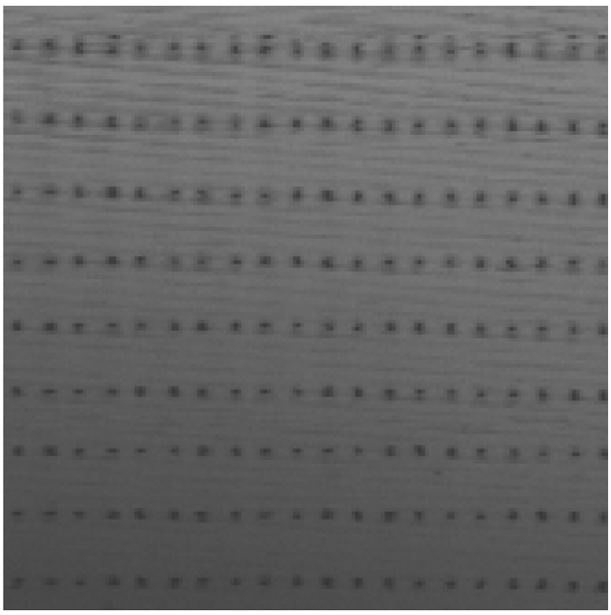

Fig. 11. Example of one-layer data storage using **3** as initiator. The distance between two adjacent bits in the layer is 5 μm.

In the experiment, the used storage medium was PMMA doped with new compounds. For example, compound **3** (99.5%) and PMMA were mixed together (with a suitable weight ratio about 1:50) in a chloroform solution, and the film was coated onto a glass slide with thickness of about 150 μm in ambient air at room temperature. There is almost no absorption above 500 nm by the chromophore; therefore, it undergoes a typical two-photon excitation on using an 820 nm femtosecond laser as the writing laser. Thus, as described in the literature [8], bits were recorded successively by a single pulse. A computer-controlled two-axis translation stage was used to move the storage medium between pulses. The recorded bits were retrieved through parallel reading with a reflection-type confocal microscope, as shown in Fig. 11. The shadow and blank can be detected and classified as stored 1 and

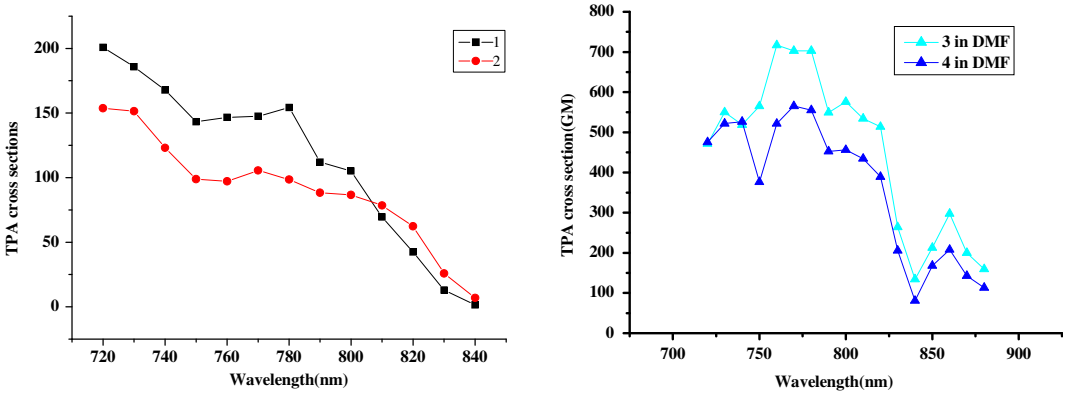

Fig. 10. Two-photon (from a 200 fs, 76 MHz Ti:sapphire laser) absorption cross sections of **1**, **2**, **3** and **4** in DMF *vs* excitation wavelengths of identical energy of 0.100 W (experimental uncertainties:10%).

0 data bits. The distance between adjacent dots in the layer was about 5 μm. The laser irradiation duration was 50 ms for each bit [25]. The difference in the bit size may be caused by the inhomogeneity of the doped chromophore in PMMA.

4. Conclusion

The synthetic methodology employing Heck and Suzuki reaction conditions facilitated a systematic variation of functional groups of differing electronic characters. The dyes show good SPEF and TPEF behavior and exhibit relatively large TPA cross section, and can be used for optical data storage when initiated at 820 nm. In this paper, the TPA properties were explored by extending the conjugation in dipolar type compounds: benzene, thiophene and vinylpyridine groups attached to a 9-hexyl-3, 6-bis(2-thienyl) carbazole unit. The results demonstrate that introduction of donor group thiophene as π electron bridge improves the two photons absorption cross sections for both A–π–D–π–A and π–σ–π type molecules greatly.

Acknowledgments

This work was supported by a grant for the National Natural Science Foundation of China (21071001, 50873001), Education committee of Anhui Province (KJ2010A030), The team for Scientific Innovation Foundation of Anhui Province (2006KJ007TD), Science and Technological Fund of Anhui Province for Outstanding Youth (10040606Y22), The 211 Project of Anhui University, Ministry of education funded projects focus on retured overseas scholar.

References

[1] (a) Abbotto A, Beverina L, Bozio R, Bradamante S, Pagani GA, Signorini R. Heterocycle-based materials for frequency-upconverted lasing. Synth Met 2001;121:1755–6;
(b) Abbotto A, Beverina L, Bozio R, Bradamante S, Ferrante C, Pagani GA, et al. Push-pull organic dyes for frequency-upconverted lasing. Adv Mater 2000;12:1963–7;
(c) Li L, Tian YP, Yang JX, Sun PP, Wu JY, Zhou HP, et al. Facile synthesis and systematic investigations of a series of novel bent-shaped two-photon absorption chromophores based on pyrimidine. Chem Asian J 2009;4:668–80;
(d) Kong L, Li WJ, Li XL, Geng WQ, Hao FY, Wu JY, et al. Four divalent metal thiocyanate coordination compounds containing a rigid functional pyridine ligand. Polyhedron 2010;29:1575–82;
(e) Zhou GJ, Wong WY. Organometallic acetylides of Pt^{II}, Au^{I} and Hg^{II} as new generation optical power limiting materials. Chem Soc Rev 2011;40:2541–66.

[2] (a) Yuan WF, Sun L, Tang HH, Wen YQ, Jiang GY, Huang WH, et al. A novel thermally stable spironaphthoxazine and its application in rewritable high density optical data storage. Adv Mater 2005;17:156–60;
(b) Jiang GY, Wang S, Yuan WF, Jiang L, Song YL, Tian H, et al. Highly fluorescent contrast for rewritable optical storage based on photochromic bisthienylethene-bridged naphthalimide dimer. Chem Mater 2006;18:235–7;
(c) Kim HM, Jeong BH, Hyon JY, An MJ, Seo MS, Hong JH, et al. Two-photon fluorescent turn-on probe for lipid rafts in live cell and tissue. J Am Chem Soc 2008;130:4246–7;
(d) Gao YH, Wu JY, Li YM, Sun PP, Zhou HP, Yang JX, et al. A sulfur-terminal Zn(II) complex and its two-photon microscopy biological imaging application. J Am Chem Soc 2009;131:5208–13;
(e) Yanez CO, Andrade CD, Yao S, Luchita G, Bondar MV, Belfield KD. Photosensitive polymeric materials for two-photon 3D WORM optical data storage systems. J Am Chem Soc 2009;1:2219–29.

[3] (a) Ehrlich JE, Wu XL, Lee IYS, Hu ZY, Röckel H, Marder SR, et al. Two-photon absorption and broadband optical limiting with bis-donor stilbenes. Opt Lett 1997;22(24):1843–5;
(b) Joel V, Gray ML, Toner M, Schmidt MA. A microfabrication-based dynamic array cytometer. Anal Chem 2002;74:3984–90;
(c) Zhao C, Burchardt M, Brinkhoff T, Beardsley C, Simon M, Wittstock G. Microfabrication of patterns of adherent marine bacterium Phaeobacter inhibens using soft lithography and scanning probe lithography. Langmuir 2010;26:8641–7.

[4] (a) Day D, Gu M, Smallridge A. Use of two-photon excitation for erasable-rewritable three-dimensional bit optical data storage in a photorefractive polymer. J Opt Lett 1999;24:948–50;
(b) Wu PL, Feng XJ, Tam HL, Wong MS, Cheah KW. Efficient three-photon excited deep blue photoluminescence and lasing of diphenylamino and 1,2,4-triazole endcapped oligofluorenes. J Am Chem Soc 2009;131:886–7;
(c) Fang HH, Chen QD, Yang J, Xia H, Gao BR, Feng J, et al. Two-photon pumped amplified spontaneous emission from cyano-substituted oligo(p-phenylenevinylene) crystals with aggregation-induced emission enhancement. J Phys Chem C 2010;114:11958–61.

[5] (a) Baur JW, Alexander JMD, Banach M, Denny LR, Reinhardt BA, Vaia RA, et al. Molecular environment effects on two-photon-absorbing heterocyclic chromophores. Chem Mater 1999;11:2899–906;
(b) Cho BR, Son KH, Lee SH, Song YS, Lee YK, Jeon SJ, et al. Two photon absorption properties of 1,3,5-tricyano-2,4,6-tris(styryl)benzene derivatives. J Am Chem Soc 2001;123:10039–45;
(c) Kogej T, Beljonne D, Meyers F, Perry JW, Marder SR, Brédas JL. Mechanisms for enhancement of two-photon absorption in donor–acceptor conjugated chromophores. Chem Phys Lett 1998;298:1–6;
(d) Albota M, Beljonne D, Brédas JL, Ehrlich JE, Fu JY, Heikal AA, et al. Design of organic molecules with large two-photon absorption cross sections. Science 1998;281:1653–6;
(e) Kannan R, He GS, Yuan LX, Xu FM, Prasad PN, Dombroskie AG, et al. Diphenylaminofluorene-based two-photon-absorbing chromophores with various ð-electron acceptors. Chem Mater 2001;13:1896–904;
(f) Adronov A, Fréchet JMJ, He GS, Kim KS, Chung SJ, Swiatkiewicz J, et al. Novel two-photon absorbing dendritic structures. Chem Mater 2000;12:2838–41;
(g) Rumi M, Ehrlich JE, Heikal AA, Perry JW, Barlow S, Hu Z, et al. Structure-property relationships for two-photon absorbing chromophores: bis-donor diphenylpolyene and bis(styryl)benzene derivatives. J Am Chem Soc 2000;122:9500–10;
(h) Moore JS. Shape-persistent molecular architectures of nanoscale dimension. Acc Chem Res 1997;30:402–13;
(i) Morales AR, Belfield KD, Hales JM, Stryland EWV, Hagan DJ. Synthesis of two-photon absorbing unsymmetrical fluorenyl-based chromophores. Chem Mater 2006;20:4972–80;
(j) Belfield KD, Morales AR, Kang BS, Hales JM, Hagan DJ, Stryland EWV, et al. Synthesis, characterization, and optical properties of new two-photon-absorbing fluorene derivatives. Chem Mater 2004;16:4634–41;
(k) Peng ZH, Pan YC, Xu BB, Zhang JH. Synthesis and optical properties of novel unsymmetrical conjugated dendrimers. J Am Chem Soc 2000;122:6619–23;
(l) Yuan Z, Entwistle CD, Collings JC, Albesa-Jové D, Batsanov AS, Howard JAK, et al. Synthesis, crystal structures, linear and nonlinear optical properties, and theoretical studies of (*p*-R-phenyl)-, (*p*-R-phenylethynyl)-, and (*E*)-[2-(*p*-R-phenyl)ethenyl] dimesitylboranes and related compounds. Chem Eur J 2006;12:2758–71;
(m) Entwistle CD, Collings JC, Steffen A, Pålsson LO, Beeby A, Albesa-Jové D, et al. Syntheses, structures, two-photon absorption cross-sections and computed second hyperpolarisabilities of quadrupolar A–π–A systems containing E-dimesitylborylethenyl acceptors. J Mater Chem 2009;19:7532–44;
(n) Collings JC, Poon SY, Droumaguet CL, Charlot M, Katan C, Pålsson LO, et al. Chem Eur J 2009;15:198–208;
(o) Jiang YH, Wang YC, Hua JL, Tang J, Li B, Qian SX, et al. Multibranched triarylamine end-capped triazines with aggregation-induced emission and large two-photon absorption cross-sections. Chem Commun 2010;46:4689–91;
(p) Wang B, Wang YC, Hua JL, Jiang YH, Huang JH, Qian SX, et al. Starburst triarylamine donor–acceptor–donor quadrupolar derivatives based on cyano-substituted diphenylaminestyryl-benzene: tunable aggregation-induced emission colors and large two-photon absorption cross sections. Chem Eur J 2011;17:2647–55;
(q) Li QQ, Huang J, Pei ZG, Zhong AS, Peng M, Liu J, et al. Synthesis and two-photon absorption properties of conjugated polymers with N-arylpyrrole as conjugated bridge and isolation moieties. J Polym Sci A Polym Chem 2011;49:2538–45;
(r) Li QQ, Huang J, Zhong AS, Zhong C, Peng M, Liu J, et al. N-arylpyrrole-based chromophores of donor-π-donor type displaying high two-photon absorption. J Phys Chem B 2011;115:4279–85.

[6] (a) Anémian R, Mulatier JC, Andraud C, Stéphan O, Vial JC. Monodisperse fluorene oligomers exhibiting strong dipolar coupling interactions. Chem Commun; 2002:1608–9;
(b) Hayek A, Nicoud JF, Bolze F, Bourgogne C, Baldeck PL. Boron-containing two-photon-absorbing chromophores: electronic interaction through the cyclodiborazane core. Angew Chem Int Ed 2006;45:6466–9.

[7] (a) Jen AKY, Rao VP, Wong KY, Drost KJ. Functionalized thiophenes: second-order nonlinear optical materials. J Am Chem Soc Chem Commmun; 1993:90–2;
(b) Guo KP, Hao JM, Zhang T, Zu FH, Zhai JF, Qiu L, et al. The synthesis and properties of novel diazo chromophores based on thiophene conjugating spacers and tricyanofuran acceptors. Dyes Pigm 2008;77:657–64;
(c) Hoegl H. On photoelectric effects in polymers and their sensitization by dopants. J Phys Chem 1965;69:755–66;
(d) Granström M, Petritsch K, Arias AC, Lux A, Andersson MR, Friend RH. Laminated fabrication of polymeric photovoltaic diodes. Nature 1998;395:257–60;
(e) Sivula K, Luscombe CK, Thompson BC, Fréchet JMJ. Enhancing the thermal stability of polythiophene:fullerene solar cells by decreasing effective polymer regioregularity. J Am Chem Soc 2006;128:13988–9;
(f) Hiorns RC, Bettignies R, Leroy J, Bailly S, Firon M, Sentein C, et al. High molecular weights, polydispersities, and annealing temperatures in the optimization of bulk-heterojunction photovoltaic cells based on

poly(3-hexylthiophene) or poly(3-butylthiophene). Adv Funct Mater 2006; 16:2263–73;
(g) Thomas KRJ, Hsu YC, Lin JT, Lee KM, Ho KC, Lai CH, et al. 2,3-Disubstituted thiophene-based organic dyes for solar cells. Chem Mater 2008;20:1830–40;
(h) Jiang YH, Wang YC, Wang B, Yang JB, He NN, Qian SX, et al. Synthesis, two-photon absorption and optical limiting properties of multibranched styryl derivatives based on 1,3,5-triazine. Chem Asian J 2011;6:157–65;
(i) Wong WY. Metallated molecular materials of fluorene derivatives and their analogues. Coord Chem Rev 2005;249:971–97;
(j) Wong WY, Ho CL. Functional metallophosphors for effective charge carrier injection/transport: new robust OLED materials with emerging applications. J Mater Chem 2009;19:4457–82;
(k) Wong WY, Ho CL. Heavy metal organometallic electrophosphors derived from multi-component chromophores. Coord Chem Rev 2009;253: 1709–58.

[8] (a) Yamasaki K, Joudkazis S, Watanabe M, Sun HB, Matsuo S, Misawa H. Recording by microexplosion and two-photon reading of three-dimensional optical memory in polymethylmethacrylate films. Appl Phys Lett 2000;76:1000–2;
(b) Day D, Gu M. Formation of voids in a doped polymethylmethacrylate polymer. Appl Phys Lett 2002;80:2404–6;
(c) Jiu HF, Tang HH, Zhou JL, Xu J, Zhang QJ, Xing H, et al. Sm(DBM)$_3$Phen-doped poly(methyl methacrylate) for three-dimensional multilayered optical memory. Opt Lett 2005;30:774–6;
(d) Li H, Xu QF, Li NJ, Sun R, Ge JF, Lu JM, et al. A small-molecule-based ternary data-storage device. J Am Chem Soc 2010;132:5542–3;
(e) Iliopoulos K, Krupka O, Gindre D, Sallé M. Reversible two-photon optical data storage in coumarin-based copolymers. J Am Chem Soc 2010;132:14343–5.

[9] (a) Zhou YJ, Chen DQ, Huang WH, Xia AD. Development of the scanning system for confocal laser scanning fluorescence microscope. Opt Precis Eng 2002;10:582–7;
(b) Jiang ZW, Zhou YJ, Yuan DJ, Huang WH, Xia AD. A two-photon femtosecond laser system for three-dimensional microfabrication and data storage. Chin Phys Lett 2003;20:2126–9;
(c) Hua JL, Li B, Meng FS, Ding F, Qian SX, Tian H. Two-photon absorption properties of hyperbranched conjugated polymers with triphenylamine as the core. Polymer 2004;45:7143–9.

[10] Strickler JH, Webb WW. Three-dimensional optical data storage in refractive media by two-photon point excitation. Opt Lett 1991;16:1780–2.

[11] Cammi R, Cossi M, Tomasi J. Analytical derivatives for molecular solutes. III. Hartree–Fock static polarizability and hyperpolarizabilities in the polarizable continuum model. J Chem Phys 1996;104:4611–20.

[12] Shen YR. The principles of nonlinear optics. New York: Wiley; 1984.

[13] Olsen J, Jørgensen P. Linear and nonlinear response functions for an exact state and for an MCSCF state. J Chem Phys 1985;82:3235–64.

[14] GAUSSIAN03 References in http://www.gaussian.com.

[15] (a) DALTON References in http://www.kjemi.uio.no/software/dalton/.
(b) Ji L, Qian SL. Effect of local feedback on Turing pattern formation. Chem Phys Lett 2004;391:176–80.

[16] (a) Zhou HP, Li DM, Zhang JZ, Zhu YM, Wu JY, Hu ZJ, et al. Crystal structures, optical properties and theoretical calculation of novel two-photon polymerization initiators. Chem Phys 2006;322:459–70;
(b) Hu ZJ, Yang JX, Tian YP, Zhou HP, Tao XT, Xu GB, et al. Synthesis and optical properties of two 2,2′:6′,2″-terpyridyl-based two-photon initiators. J Mol Struct 2007;839:50–7;
(c) He GS, Lin TC, Chung SJ, Zheng QD, Lu CG, Cui YP, et al. Two-, three-, and four-photon-pumped stimulated cavityless lasing properties of ten stilbazolium-dyes solutions. J Opt Soc Am B 2005;22:2219–28.

[17] MOLEKEL, references in http://www.cscs.ch/molekel/.

[18] (a) Jenekhe SA, Lu LD, Alam MM. New conjugated polymers with donor-acceptor architectures: synthesis and photophysics of carbazole-quinoline and phenothiazine-quinoline copolymers and oligomers exhibiting large intramolecular charge transfer. Macromolecules 2001;34:7315–24;
(b) Breitung EM, Shu CF, McMahon RJ. Thiazole and thiophene analogues of donor-acceptor stilbenes: molecular hyperpolarizabilities and structure–property relationships. J Am Chem Soc 2000;122:1154–60;
(c) Heeney M, Bailey C, Genevicius K, Shkunov M, Sparrowe D, Tierney S, et al. Stable polythiophene semiconductors incorporating thieno[2,3-b]thiophene. J Am Chem Soc 2005;127:1078–9;
(d) Brocks G. Density functional study of polythiophene derivatives. J Phys Chem 1996;100:17327–33.

[19] Liu ZQ, Fang Q, Cao DX, Wang D, Xu GB. Triaryl boron-based A-π-A vs triaryl nitrogen-based D-π-D quadrupolar compounds for single- and two-photon excited fluorescence. Org Lett 2004;6:2933–6.

[20] (a) Agrawal AK, Jenekhe SA. New conjugated polyanthrazolines containing thio-phene moieties in the main chain. Macromolecules 1991;24: 6806–8;
(b) Agrawal AK, Jenekhe SA. New series of conjugated rigid-rod polyquinolines and polyanthrazolines. Macromolecules 1993;26:895–905;
(c) Agrawal AK, Jenekhe SA. Synthesis and processing of heterocyclic polymers as electronic, optoelectronic, and nonlinear optical materials. New conjugated polyquinolines with electron-donor or-acceptor side groups. Chem Mater 1993;5:633–40;
(d) Cui YT, Zhang XJ, Jenekhe SA. Thiophene-linked polyphenylquinoxaline: a new electron transport conjugated polymer for electroluminescent devices. Macromolecules 1999;32:3824–6;
(e) Agrawal AK, Jenekhe SA. Electrochemical properties and electronic structures of conjugated polyquinolines and polyanthrazolines. Chem Mater 1996;8:579–89;
(f) Dorcas MMF, George F, Alan JL, Christopher G. Chiral *versus* racemic building blocks in supra-molecular chemistry: tartrate salts of organic diamines. Acta Cryst 2002;B58:272–88.

[21] (a) Kessler MA, Wolfbeis OS. New highly fluorescent ketocyanine polarity probes. Spectrochim Acta A 1991;47:187–92;
(b) Srividya N, Ramamurthy P, Ramkrishnan VT. Solvent effects on the absorption and fluorescence spectra of some acridinedione dyes: determination of ground and excited state dipole moments. Spectrochim Acta A 1997; 53:1743–53.

[22] Grabowski ZR, Rotkiewicz K, Retting W. Structural changes accompanying intramolecular electron transfer: focus on twisted intramolecular charge-transfer states and structures. Chem Rev 2003;103:3899–4032.

[23] Tian YP, Li L, Zhang JZ, Yang JX, Zhou HP, Wu JY, et al. Investigations and facile synthesis of a series of novel multi-functional two-photon absorption materials. J Mater Chem 2007;17:3646–54.

[24] Harpham MR, Süzer ö, Ma CQ, Bäuerle P, Goodson T. Tri-aryl boron-based A-π-A vs tri-aryl nitrogen-based D-π-D quadrupolar compounds for single & two-photon excited fluorescence. J Am Chem Soc 2009;131:973–9.

[25] Zhou YJ, Tang HH, Huang WH. Three-dimensional optical data storage in a novel photochromic material with two-photon writing and one-photon readout. Opt Eng 2005;44:0352021–5.